

Manipulating the motion of a single atom in a standing wave via feedback

J. A. Dunningham, H. M. Wiseman, and D. F. Walls

Department of Physics, University of Auckland, Auckland, New Zealand

(Received 8 July 1996)

A standing light wave appears to a highly detuned two-level atom as a sinusoidal potential. This causes the atoms to be channeled to the minima of the potentials. At the same time, the atom changes the phase of the light field. Detecting this phase shift yields information about the position of the atom. In this paper we show that this information may be used to control the intensity of the light field so as to modify the effective shape of the potential “seen” by the atom. Our numerical simulations show that the effectiveness of the channeling may be significantly enhanced by such quantum-limited feedback. We discuss possible applications to atom lithography. [S1050-2947(97)00502-7]

PACS number(s): 42.50.Dv, 42.50.Lc, 03.65.Bz

I. INTRODUCTION

It is well known that a highly detuned light field acts as a scalar potential for a two-level atom [1]. The force from this potential is known as the dipole force and is proportional to the intensity gradient of the field. A standing wave in an optical cavity thus appears to a first approximation as a series of potential hills and valleys that channel the atoms. Channeling has been shown to occur in the vicinity of the nodes if the laser field is blue detuned ($\Delta > 0$) from the atomic resonance and near the antinodes for red detuning ($\Delta < 0$) [2]. This channeling could be applied in atomic lithography, as the laying down of a series of lines on a substrate has been demonstrated experimentally using chromium atoms [3]. There are many reasons why such atomic deposition is imperfect, but one fundamental limit is that the potential wells created by the standing wave are sinusoidal rather than harmonic [4].

Although the dominant physical effect of placing an atom in a standing wave is the dipole force on the atom, the field is also affected. That is because there is a small but not necessarily negligible refractive index due to a single atom. This causes the phase of the light to be shifted, and the amount of this shift depends on the position of the atom. The phase shift is zero for the atom at a node and maximal at an antinode. It has been shown theoretically that this phase shift can be used to make a quantum-limited measurement of the position (modulo half a wavelength) of an atom by passing it through a standing wave for a time sufficiently short for its transverse motion to be negligible [5]. More recently it has also been shown theoretically that one can track the oscillatory motion of an atom in a standing wave by continually monitoring the phase of the field using homodyne detection [6].

In this paper we draw together these two aspects of the interaction of an atom with a detuned standing wave in a different proposal. On the quantum optics side we take the monitoring of the atom’s position one step further by considering the continuous feedback of the homodyne photocurrent to influence the atom’s future evolution. On the atom optics side we show that this feedback can be used to improve the degree of channeling in atomic lithography. This is done by modifying the effective potential the atom “sees” to be

closer to harmonic rather sinusoidal. The basic idea is that whatever position for the atom is indicated by the measurement, the intensity of the field is modified so that the local potential seen by the atom is that of a parabola. The curvature of the parabola is chosen to fit with the sinusoid that the atom sees in the absence of feedback, near the base of the potential wells. This is an interesting application of the quantum theory of feedback because, unlike most previous applications, it produces a substantial change in the system dynamics [7].

In order to find the ultimate limits to atom channeling by this method we have done a fully quantum-mechanical treatment of the atomic motion. In Sec. II we derive our model of the atom in the standing wave with feedback. To simplify the calculation we adiabatically eliminate the field, but the vacuum fluctuations entering into the cavity (necessary in order to extract information from the light) still affect the atom and are manifest as back-action noise terms in the Hamiltonian. In addition to this, the feedback also introduces noise into the system, due to the homodyne photocurrent shot noise [7,8]. As expected, the more we modify the potential, the more noise we introduce. The question arises whether modifying the potential (and taking into account the noise that we inevitably introduce) gives improved localization over the case with no feedback. In order to answer this we present in Sec. III the results of numerical simulations comparing four cases: (i) no feedback, (ii) linear feedback (LF), (iii) nonlinear feedback (NLF), and (iv) linear feedback with an optical nonlinearity (LFON). Our results show that feedback (and particularly nonlinear feedback) can potentially improve channeling beyond the standard quantum limit with no feedback. In Sec. IV we discuss experimental practicalities and Sec. V concludes.

II. THEORY

A. Conservative motion

The starting point for our theory is the Hamiltonian describing the coupling between a two-level atom and a single-mode electromagnetic standing wave inside a cavity. We denote the position of the atom (along the cavity axis) by z and its momentum in this direction by p . The one-photon Rabi frequency is denoted Ω and the detuning of the atom Δ . The

atom lowering operator is σ and the field annihilation operator is a . Then the Hamiltonian is

$$H = \frac{p^2}{2} + \Omega \sin z (a^\dagger \sigma + a \sigma^\dagger) + \Delta \sigma^\dagger \sigma. \quad (2.1)$$

Here we are using atom optics units

$$\hbar = M = \frac{\lambda}{2\pi} = 1, \quad (2.2)$$

where M is the mass of the atom and λ the wavelength of the light. For example, in these units the recoil frequency (or energy) is $1/2$.

Now we assume that the atom is highly blue detuned, with $|\Delta|$ much greater than all other rates. This is necessary to avoid spontaneous emission. The atom will then remain in the ground state and may be treated as a scalar particle with the effective Hamiltonian [9]

$$H = \frac{p^2}{2} + g a^\dagger a S(z), \quad (2.3)$$

where z is the unitless ratio of the position along the cavity axis to the laser wavelength. Here we are using $g = \Omega^2/|\Delta|$ and also

$$S(z) \equiv \sin^2(z). \quad (2.4)$$

As far as the field is concerned, the second term represents a detuning that depends on the position of the atom. As far as the atom is concerned, the field intensity gives a potential. In this section we are interested only in this effect on the atom so that we treat the field classically by replacing $a^\dagger a$ with $|\alpha|^2$. This gives a conservative atomic Hamiltonian

$$H_{\text{cons}} = \frac{p^2}{2} + \frac{\omega^2}{2} S(z), \quad (2.5)$$

where $\omega^2 = 2g|\alpha|^2$.

Near $z=0$ this Hamiltonian is approximated by

$$H_{\text{cons}} \approx \frac{p^2}{2} + \frac{\omega^2}{2} z^2, \quad (2.6)$$

which is that of a harmonic oscillator. Clearly ω is the frequency of oscillation of an atom near the bottom of the potential wells. Now, since $S(z) \leq 1$, the maximum height of the potential wells is $\omega^2/2$, so that the number of energy levels per well is of order ω [10]. Thus ω is a measure of the classicality of the problem, in that for $\omega \gg 1$ the atom dynamics should be well approximated by classical dynamics for times long compared to ω^{-1} [11].

The defining property of a harmonic oscillator is of course that its dynamics is characterized by a single frequency ω . This has the following consequence. If a classical ensemble of atoms were to enter a region of space where the potential was harmonic, as in Eq. (2.6), with an initial momentum of zero, then after exactly one-quarter of a period all of the atoms will have $z=0$. Quantum mechanically, if at $t=0$ the atomic wave function is in the zero-momentum eigenstate, at $t = \pi/2\omega$ it will be in the zero-position eigenstate. Of course

with the true potential of Eq. (2.5) this will not occur. Nevertheless, we expect that at this time the atomic position distribution will become peaked at the nodes of the standing wave, where $z = n\pi$ for n an integer. This is the essence of the idea behind channeling of atoms.

B. Continuous observation

As stated in the Introduction, we wish to consider manipulating the motion of the atoms by feedback. In order to do this we first need to consider measurement of the position of the atom. This is possible because the position of the atom is coupled to the phase of the field, which is something that can be observed. Here, as in Ref. [6], we want to continuously monitor the phase of the field in order to find out about the position of the atom. The easiest way to monitor the phase of the field is to give the cavity a finite intensity damping rate of κ . In fact, such cavity loss is unavoidable. With a leaky cavity, in order to maintain a constant intensity of light inside the cavity (and hence a constant potential for the atom) it is necessary to drive that cavity. This can be done by shining a laser into the lossy mirror. We model this by having the input field (in the sense of Gardiner and Collett [12]) given by

$$b_{\text{in}}(t) = \sqrt{\kappa} \frac{-i\alpha}{2} + \nu(t). \quad (2.7)$$

Here α is a real dimensionless coherent amplitude and $b_{\text{in}}(t)$ is normalized such that the photon flux is $\langle b_{\text{in}}^\dagger(t) b_{\text{in}}(t) \rangle = \kappa |\alpha|^2/4$. The other term $\nu(t)$ is operator-valued white noise [12] of zero mean obeying

$$[\nu(t), \nu^\dagger(t')] = \delta(t-t') = \langle \nu(t) \nu^\dagger(t') \rangle, \quad (2.8)$$

where this last expression is the unique nonvanishing second-order moment. It can be thought of as vacuum fluctuations, which can be decomposed into two statistically independent but noncommuting quadratures

$$\xi(t) = \nu(t) + \nu^\dagger(t), \quad \nu(t) = -i[\nu(t) - \nu^\dagger(t)] \quad (2.9)$$

satisfying

$$\langle \xi(t) \xi(t') \rangle = \langle \nu(t) \nu(t') \rangle = \delta(t-t'). \quad (2.10)$$

The Hamiltonian including the coupling of the cavity mode to the external field is [12,8]

$$H_{\text{damped}} = \frac{p^2}{2} + g a^\dagger a S(z) - i\sqrt{\kappa} [b_{\text{in}}(t) a^\dagger + a b_{\text{in}}^\dagger(t)]. \quad (2.11)$$

Up until now our approach has been similar to that of Ref. [6], although we have made an additional approximation in adiabatically eliminating the upper state of the atom. However, in order to keep the problem tractable we wish to make the substantial further approximation of eliminating the field. This will be valid provided that κ is sufficiently large. To do this we first obtain the Heisenberg equation for the field operator a . Treating the noise terms in Eq. (2.11) carefully yields the following Itô equation for a :

$$\dot{a} = -\frac{\kappa}{2}a - \sqrt{\kappa}b_{\text{in}}(t) - igS(z)a. \quad (2.12)$$

Assuming κ to be large, we can set the time derivative in Eq. (2.12) to zero, obtaining

$$a \approx \frac{i\alpha - 2\nu(t)/\sqrt{\kappa}}{1 + 2igS(z)/\kappa}. \quad (2.13)$$

Strictly this expression cannot be true because $\nu(t)$ has white-noise fluctuations so that it is impossible for a to relax fast enough to be slaved to the vacuum noise. However, if we interpret the noise term as vacuum fluctuations restricted to the bandwidth κ , then they can be thought of as finite, and even small compared to $\alpha \gg 1$. Therefore, it is appropriate to linearize the expression for $a^\dagger a$ to get

$$a^\dagger a \approx \frac{|\alpha|^2 - 2\alpha\nu(t)/\sqrt{\kappa}}{1 + [2gS(z)/\kappa]^2}. \quad (2.14)$$

Now if $(g/\kappa)^2 \ll 1$, the second term in the denominator may be ignored, making $a^\dagger a$ independent of the position of the atom. This allows the expression for $a^\dagger a$ to be simply substituted into Eq. (2.3) to yield the effective Hamiltonian for the atom alone

$$H_{\text{meas}} = \frac{p^2}{2} + \frac{\omega^2}{2}S(z) \left(1 - \frac{2\nu(t)}{\alpha\sqrt{\kappa}} \right). \quad (2.15)$$

This does not involve any operators for the cavity mode, but it does involve a noise operator from the external vacuum fluctuations. The effect of that noise is to produce a noisy potential for the atom. This will of course disturb the momentum of the atom, as it gives rise to the term

$$\dot{p}_{\text{disturbance}} = i \left[-\frac{\omega^2}{2}S(z) \frac{2\nu(t)}{\alpha\sqrt{\kappa}}, p \right] \quad (2.16)$$

$$= g\alpha 2\sin 2z \nu(t)/\sqrt{\kappa}. \quad (2.17)$$

Consider a short time $t_1 \ll \omega^{-1}$. This allows one to use the Raman-Nath approximation [13] of neglecting the kinetic-energy term so that the position of the atom remains constant. Over this short time t_1 the noisy evolution (2.16) will result in a mean-square disturbance of the atom's momentum of

$$(\delta p)_{\text{disturbance}}^2 = 4g^2\alpha^2 t_1 \langle \sin^2 2z \rangle / \kappa. \quad (2.18)$$

This disturbance can be ascribed to the Heisenberg uncertainty relation as follows. The damping of the cavity gives an output field that may be measured

$$b_{\text{out}}(t) = b_{\text{in}}(t) + \sqrt{\kappa}a \quad (2.19)$$

$$\approx -\sqrt{\kappa}[\nu(t)/\sqrt{\kappa} - i\alpha/2 - 2gS(z)\alpha/\kappa]. \quad (2.20)$$

As stated above, we wish to measure the phase of the field. This can be done by doing a homodyne measurement of the phase quadrature of the output. The resultant photocurrent, suitably normalized, is

$$I_{\text{hom}}(t) = \sqrt{\kappa}[b_{\text{out}}(t) + b_{\text{out}}^\dagger(t)] \quad (2.21)$$

$$= 4gS(z)\alpha - \sqrt{\kappa}\xi(t). \quad (2.22)$$

This contains a term proportional to $S(z)$, which gives information about the position of the atom, plus a noise term. Over a time t_1 within the Raman-Nath regime as above, one's best estimate for $S(z)$ is obviously

$$\hat{S} = \frac{1}{t_1} \int_0^{t_1} \frac{I_{\text{hom}}(t)}{4g\alpha} dt. \quad (2.23)$$

Note that we are using a circumflex to denote an experimental estimate of a quantity, not an operator.

The experimental error in \hat{S} , as opposed to intrinsic uncertainty in $S(z)$, is determined by

$$(\delta \hat{S})_{\text{error}}^2 = \left\langle \left(\frac{1}{t_1} \int_0^{t_1} \frac{\sqrt{\kappa}\xi(t)}{4g\alpha} dt \right)^2 \right\rangle \quad (2.24)$$

$$= \frac{\kappa}{16g^2\alpha^2 t_1}. \quad (2.25)$$

Thus we can derive the relation

$$(\delta \hat{S})_{\text{error}}^2 (\delta p)_{\text{disturbance}}^2 = \frac{1}{4} \langle \sin^2 2z \rangle. \quad (2.26)$$

This equality is *precisely* the minimum expected from Robertson's generalization [14] of Heisenberg's uncertainty principle, given the commutator

$$[S(z), p] = i\sin 2z. \quad (2.27)$$

Of course the atom's momentum will be disturbed by the amount (2.18) regardless of whether the experimenter undertakes a homodyne measurement of the outgoing field in order to obtain information about the atom's positions. Nevertheless, it is the fact that the experimenter can obtain such information, with experimental error $\delta \hat{S}_{\text{error}}$, which implies that the momentum must be disturbed by at least the $\delta p_{\text{disturbance}}$ of Eq. (2.18). The more accurately one wishes to know the position (in a given time t_1) the more noise one will necessarily add to the atom's momentum. This will have important consequences when we consider feeding back the information in $I_{\text{hom}}(t)$, in subsequent sections.

C. Linear feedback

In this section we introduce feedback into our system. The motivation behind the feedback is, as explained in the Introduction, to change the effective potential shape the atom sees from sinusoidal to something that is closer to a periodic array of parabolas, as shown in Fig. 1. Near $z = n\pi$, these parabolas match the minima of the sinusoid, but away from the minima the sinusoid falls short of the parabola. In order to make the atom see a more parabolic shape, one would wish

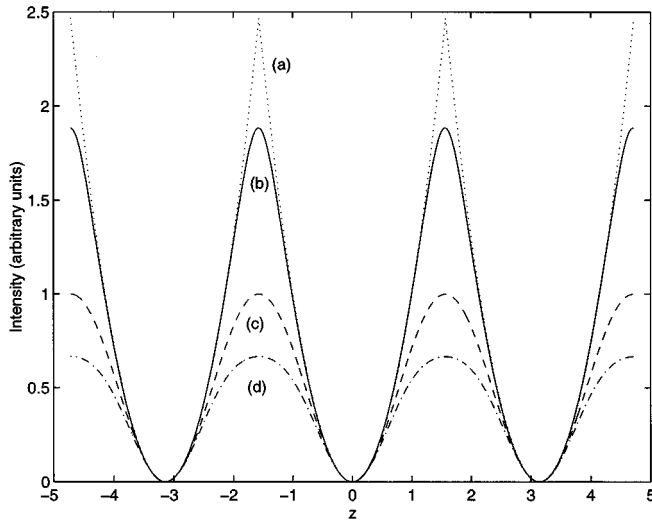


FIG. 1. Diagram of the (a) pseudoharmonic potential as a function of the position along the cavity axis z (in units of the laser wavelength). Also shown are the (b) nonlinear feedback [see below Eq. (3.13)], (c) linear feedback [see Eq. (2.43)], and (d) unmodified sinusoidal potentials.

to increase the intensity of the light (and hence the height of the sinusoid) if the atom is away from the potential minima, but leave it unchanged if it is near the minima. This information (the displacement of the atom away from the potential minima) is encoded in the operator $S(z)$. Furthermore, this operator can be estimated (with finite accuracy of course) from the homodyne photocurrent $I_{\text{hom}}(t)$, as shown in Sec. II B. By feeding back the information in $I_{\text{hom}}(t)$ to control the intensity of the light, one could hope to modify the motion of the atom to good effect. To model this quantum-limited feedback we use the quantum Langevin approach rather than the quantum trajectory approach [8].

To simplify the problem, we assume that the feedback is Markovian. That is to say, we assume that the response function of the feedback loop is approximately flat from zero to a frequency much larger than that of the atomic evolution ω . Furthermore, in this section, we assume that the intensity of the cavity mode is controlled by varying the amplitude of the driving linearly with the instantaneous photocurrent, as shown in Fig. 2. This can be achieved using electro-optic polarization modulators and polarization-sensitive beam splitters [15]. This feedback can be modeled simply by changing the input beam from Eq. (2.7) to

$$b_{\text{in}}(t) = \frac{-i\sqrt{\kappa}}{2} \left[\alpha + \lambda \frac{I_{\text{hom}}(t)}{\kappa} \right] + \nu(t), \quad (2.28)$$

where λ is a dimensionless quantity whose magnitude is yet to be determined. However, we expect that the best value of λ will be positive, as this will lead to an increased driving when the atom is estimated to be far from a potential minima [when $S(z)$ is large and hence $I(t)$ is expected to be positive].

As in Sec. II B, we wish to eliminate the internal field from the problem. It is necessary to include the cavity field to begin with, however, because the feedback acts on this field, not directly on the atom. Once the feedback has been

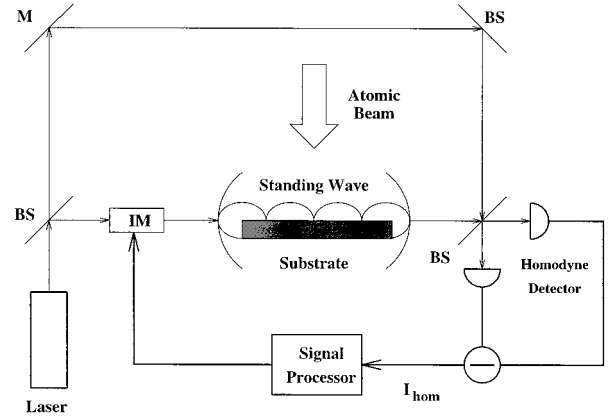


FIG. 2. Setup used for the feedback scheme. A homodyne detector is used to make a phase measurement of the output b_{out} from the cavity giving information about the transverse position of the atom in the light field. The homodyne current I_{hom} is fed into a signal processor and the output is some function of I_{hom} depending on the sort of feedback under study. This output is used to vary the amplitude of the driving b_{in} of the optical cavity. Although this appears to differ from the description given in the text, which was for a one-sided cavity, this arrangement is equivalent providing the loss rate at the driving (left) mirror is much less than that at the detection (right) mirror.

included, we can then proceed to eliminate the field to discover the effect of the feedback on the atom alone. The field obeys the same equation as before [Eq. (2.12)], but with the modified $b_{\text{in}}(t)$. For convenience we introduce the quadratures of the field

$$x = a + a^\dagger, \quad y = -i(a - a^\dagger). \quad (2.29)$$

In terms of these the homodyne photocurrent is given by

$$I_{\text{hom}}(t) = \kappa x + \sqrt{\kappa} \xi(t). \quad (2.30)$$

Substituting this into Eq. (2.28) and that into Eq. (2.12) and separating into the quadratures yields

$$\dot{x} = -\frac{\kappa}{2}x - \sqrt{\kappa}\xi(t) + gS(z)y, \quad (2.31)$$

$$\dot{y} = -\frac{\kappa}{2}y - \sqrt{\kappa}\nu(t) + \kappa\alpha + \kappa\lambda[x + \xi(t)/\sqrt{\kappa}] - gS(z)x. \quad (2.32)$$

Ignoring terms of order $(g/\kappa)^2$, as in Sec. II B, we find the stationary solutions to be

$$\frac{x}{2} \approx \left[1 - \frac{4\lambda S(z)g}{\kappa} \right]^{-1} \left[-\frac{\xi(t)}{\sqrt{\kappa}} + \frac{\alpha g S(z)}{\kappa} \right], \quad (2.33)$$

$$\frac{y}{2} \approx \left[1 - \frac{4\lambda S(z)g}{\kappa} \right]^{-1} \left[\alpha - \frac{\nu(t) + \lambda \xi(t)}{\sqrt{\kappa}} \right]. \quad (2.34)$$

These are the same as the previously derived expression for a [Eq. (2.13)] apart from the term proportional to λ in the denominator. This denominator is still of order one if λ is of order one (as will be chosen) because $S(z)$ is bounded above

by unity and g/κ is small. Thus the total decay rate is still of order κ as required for the adiabatic elimination. The purpose of the elimination is to find an expression for $a^\dagger a$ in terms of external field operators and atom operators. Linearizing the noise terms we find

$$a^\dagger a \approx (y/2)^2 \quad (2.35)$$

$$\approx \left[1 - \frac{4\lambda S(z)g}{\kappa} \right]^{-2} \left[|\alpha|^2 - 2\alpha \frac{v(t) + \lambda \xi(t)}{\sqrt{\kappa}} \right]. \quad (2.36)$$

In this case the expression for $a^\dagger a$ does depend on the atom's position. This is as desired for the feedback to work, but it means that we cannot simply substitute it into Eq. (2.3). As a field operator, $a^\dagger a$ should commute with all atomic operators, but the above expression (2.36) does not. This apparent contradiction is because the atomic operators in Eq. (2.36) should strictly be evaluated at a slightly earlier time, even under the Markovian approximation for the feedback. The consistent procedure is to use Eq. (2.3) to generate the force on the atom, treating $a^\dagger a$ as a field operator, and then to substitute in the expression for $a^\dagger a$ [Eq. (2.36)] in terms of the atomic operators, that is,

$$F(z) \equiv i[H, p] \quad (2.37)$$

$$= -g a^\dagger a S'(z) \quad (2.38)$$

$$\approx -g \frac{S'(z)}{[1 - \beta S(z)]^2} \left[|\alpha|^2 - 2\alpha \frac{v(t) + \lambda \xi(t)}{\sqrt{\kappa}} \right]. \quad (2.39)$$

Here we have defined

$$\beta = 4\lambda g/\kappa \quad (2.40)$$

and a prime denotes differentiation. Now we define the effective potential for determining the atom's motion to be

$$\begin{aligned} V_{\text{LF}}(z) &\equiv - \int_0^z d\zeta F(\zeta) \\ &= \frac{S(z)}{1 - \beta S(z)} \left\{ \frac{\omega^2}{2} - \sqrt{\frac{\omega^2 \beta}{2}} \left[\frac{v(t)}{\sqrt{\lambda}} + \xi(t) \sqrt{\lambda} \right] \right\}, \end{aligned} \quad (2.41)$$

where we are using $\omega^2 = 2g|\alpha|^2$ as before.

Evidently, the effect of the feedback is to change the shape of the potential the atom sees, as desired. To find out what feedback strength should be chosen we expand the deterministic part of the new potential around $z=0$ to find

$$\langle V_{\text{LF}}(z) \rangle \approx \frac{\omega^2}{2} [z^2 - z^4/3 + \beta z^4 + O(z^6)]. \quad (2.42)$$

Obviously we wish to choose $\beta=1/3$ in order to make the linear feedback potential closer to harmonic. This implies $g/\kappa = (12\lambda)^{-1}$. It is also apparent from Eq. (2.41) that the feedback has introduced extra noise into the potential. In addition to the disturbance of the momentum due to the measurement of position, proportional to $v(t)$, there is the noise due to the error in the measurement of position, proportional

to $\xi(t)$, being fed back due to the modification of the potential. As noted in Sec. II B, the magnitude of these noises are reciprocally related because an accurate measurement of position implies a large disturbance of the momentum. In Eq. (2.41) this uncertainty principle is manifest in that the measurement back-action noise scales as $1/\lambda$, while the fed-back measurement error scales as λ . Clearly the minimum overall noise is when $\lambda=1$. This implies $g/\kappa=1/12$, so the above approximation of ignoring terms of order $(g/\kappa)^2=1/144$ seems quite reasonable. The final expression for the atomic Hamiltonian from linear feedback is

$$H_{\text{LF}} = \frac{p^2}{2} + \frac{S(z)}{1 - S(z)/3} \left\{ \frac{\omega^2}{2} - \sqrt{\frac{\omega^2}{6}} \left[\frac{v(t) + \xi(t)}{\sqrt{6}} \right] \right\}. \quad (2.43)$$

The shape of the deterministic part of the potential is shown in Fig. 1(c).

Validity of the linear feedback Hamiltonian

In the above adiabatic elimination of the field we have assumed first that the cavity decay rate is large compared to the rate of change of the atomic position. That is to say, we require

$$\omega \ll \kappa. \quad (2.44)$$

A more subtle requirement is that the linearization of $a^\dagger a$ be valid. This requires that we can regard the white-noise terms as small compared to the coherent amplitude α . To do this we have to imagine averaging over some time t_2 such that

$$\frac{2}{\kappa t_2} \ll \alpha^2, \quad (2.45)$$

which gives

$$\frac{1}{t_2} \ll 6\omega^2. \quad (2.46)$$

Now the elimination of the field can only be valid if the atom does not move significantly during this averaging time. This requires

$$\omega \ll \frac{1}{t_2} \ll 6\omega^2. \quad (2.47)$$

The final condition is therefore

$$\omega \gg \frac{1}{6}. \quad (2.48)$$

This indicates that the linear feedback Hamiltonian is not valid in the very strong quantum regime, where ω is of order one.

D. Nonlinear feedback

In the preceding subsection we showed how varying the driving field linearly with the photocurrent from the phase

quadrature measurement of the field can lead to an effective potential for the atom that is considerably closer to pseudoharmonic than the original sinusoid. By pseudoharmonic we mean a periodic potential consisting of harmonic potentials repeated every half wavelength. In this section we show that by feeding back a nonlinear function of the photocurrent one can in principle produce an effective atomic potential that is arbitrarily close to pseudoharmonic.

As above, we model the feedback as a modulation of the coherent amplitude of the driving field, but this time we set

$$b_{\text{in}}(t) = \frac{-i\sqrt{\kappa}}{2} \left[\alpha + h \left(\frac{I_{\text{hom}}(t)}{\kappa} \right) \right] + \nu(t), \quad (2.49)$$

where h is a function that is to be determined. Now because $I_{\text{hom}}(t)$ contains a white-noise term, this expression only makes sense if the photocurrent is interpreted as a time-averaged photocurrent such that the fluctuations in it are small. For this reason we must use

$$h \left(\frac{I_{\text{hom}}(t)}{\kappa} \right) \approx h(\bar{x}) + h'(\bar{x}) [\delta x(t) + \xi(t)/\sqrt{\kappa}], \quad (2.50)$$

where $\delta x(t)$ are the rapid fluctuations in the field quadrature due to the vacuum noise inputs and \bar{x} is the mean value of x . Note, however, that \bar{x} will still be an operator in that it depends on the assumed slowly varying atomic operator $S(z)$.

Using this linearization yields the following expression for the rapid fluctuations in the field quadratures:

$$\dot{\delta x} = -\frac{\kappa}{2} \delta x - \sqrt{\kappa} \xi(t) + g S(z) \delta y, \quad (2.51)$$

$$\dot{\delta y} = -\frac{\kappa}{2} \delta y - \sqrt{\kappa} \nu(t) + \kappa h'(\bar{x}) [\delta x + \xi(t)/\sqrt{\kappa}], \quad (2.52)$$

while the mean values obey the nonlinear equations

$$\bar{x} = 2r S(z) \bar{y}, \quad (2.53)$$

$$\bar{y} = 2\alpha + 2h(\bar{x}), \quad (2.54)$$

where we have neglected terms of order $r^2 \equiv (g/\kappa)^2$ as above. Substituting the first of these into the second yields

$$h(2r S(z) \bar{y}) = -\alpha + \bar{y}/2. \quad (2.55)$$

Now say that we wish to use this feedback to create a mean force on the atom that is of the form

$$\langle F_{\text{NLF}}(z) \rangle = -\omega^2 v(z), \quad (2.56)$$

where $v(z)$ is a periodic function obeying

$$v(z) = v(z + \pi) = -v(-z). \quad (2.57)$$

From the procedure used for linear feedback it is apparent that to achieve this we require

$$\overline{a^\dagger a S'(z)} \approx \left(\frac{\bar{y}}{2} \right)^2 S'(z) = 2\alpha^2 v(z); \quad (2.58)$$

in other words,

$$\bar{y} = 2\alpha f(z), \quad (2.59)$$

where we have defined

$$f(z) \equiv \sqrt{\frac{2v(z)}{S'(z)}}. \quad (2.60)$$

Substituting this into Eq. (2.55) yields

$$h(4r\alpha S(z)f(z)) = \alpha[f(z) - 1]. \quad (2.61)$$

Differentiating both sides with respect to z gives

$$h'(4r\alpha S(z)f(z)) 4r\alpha [S'(z)v(z) + S(z)v'(z)] = \alpha f'(z). \quad (2.62)$$

Thus

$$l(z) \equiv h'(\bar{x}(z)) = h'(4r\alpha S(z)f(z)) \quad (2.63)$$

$$= \frac{f'(z)}{4r[S'(z)f(z) + S(z)f'(z)]}. \quad (2.64)$$

Now from Eq. (2.52) we have

$$\frac{\delta y}{2} = -[1 - 4rl(z)S(z)]^{-1} [\nu(t) + l(z)\xi(t)]/\sqrt{\kappa}. \quad (2.65)$$

Therefore

$$a^\dagger a \approx \frac{\bar{y}^2 + 2\bar{y}\delta y}{4} \quad (2.66)$$

$$\approx \alpha^2 [f(z)]^2 - \frac{2\alpha f(z) [\nu(t) + l(z)\xi(t)]}{\sqrt{\kappa} [1 - 4rl(z)S(z)]} \quad (2.67)$$

and the force on the atom is

$$F(z) = -g S'(z) a^\dagger a \quad (2.68)$$

$$\approx -\omega^2 v(z) + \omega \sqrt{2r} S'(z) f(z) \frac{\nu(t) + l(z)\xi(t)}{1 - 4rl(z)S(z)}. \quad (2.69)$$

The effective potential for the atom is again

$$V_{\text{NLF}}(z) = -\int_0^z d\xi F(\xi). \quad (2.70)$$

If the atom's position z is close to a node (e.g., $z=0$) then the feedback need not operate in order to make the potential harmonic. In our theory this statement amounts to saying that $v(z) \approx z$ for $z \approx 0$. In that case we find $f(z) = 1 - z^2/3 + O(z^4)$ and so

$$l(z) \rightarrow (12r)^{-1} \quad \text{as } z \rightarrow 0. \quad (2.71)$$

It is then evident from Eq. (2.68) that the overall noise is minimized when $r = 1/12$, at least near $z = n\pi$, as found in

Sec. II C. Assuming that this small value for r gives the total expression for the effective Hamiltonian for the atom with nonlinear feedback,

$$H_{\text{NLF}} = \frac{p^2}{2} + \frac{\omega^2}{2} V_0(z) - \sqrt{\frac{\omega^2}{6}} [V_1(z)\xi(t) + V_2(z)v(t)]. \quad (2.72)$$

Here the three integrals

$$V_0(z) = \int_0^z d\zeta 2v(\zeta), \quad (2.73)$$

$$V_1(z) = \int_0^z d\zeta S'(\zeta)f(\zeta)l(\zeta)[1-l(\zeta)S(\zeta)/3]^{-1}, \quad (2.74)$$

$$V_2(z) = \int_0^z d\zeta S'(\zeta)f(\zeta)[1-l(\zeta)S(\zeta)/3]^{-1} \quad (2.75)$$

in general have to be evaluated numerically up to $z = \pi/2$.

One case of great interest is for

$$v(z) = \tilde{z} \equiv z \bmod \pi \in (-\pi/2, \pi/2), \quad (2.76)$$

for which the effective potential will be exactly pseudoharmonic. Then from Eq. (2.60) we find that as $z \rightarrow \pi/2$, $f(z)$ has a simple pole and $f'(z)$ a double pole. But Eq. (2.62) implies that

$$4rl(z)[S'(z)f(z) + S(z)f'(z)] = f'(z). \quad (2.77)$$

Since $S'(z) \sim (z - \pi/2)$ near $z = \pi/2$, we find that $4rl(z)S(z) - 1 \sim (z - \pi/2)^2$. That is to say, for any value of r , the integrand in the noise terms $V_1(z), V_2(z)$ has a double pole at $z = \pi/2$. The noise terms themselves therefore have a simple pole at this position. This infinite noise is easily understood from the following argument. At $\tilde{z} = \pm \pi/2$, $S(z)$ is flat as a function of z . That is to say, the photocurrent [which measures $S(z)$] is very insensitive to changes in z . Yet in order for the feedback to change the sinusoidal potential into a pseudoharmonic potential it is necessary to use an estimate for z since $V_0(z) = \tilde{z}^2$ is not flat as a function of z near the peaks. Thus, for z near $(n+1/2)\pi$ the feedback function $h(x)$ must be very sensitive to small changes in the photocurrent. As the signal becomes weak the proportion of noise being fed back increases to the point where the noise is infinite at $z = (n+1/2)\pi$. At this point the approximations made in the above derivation clearly break down. The denominator in Eq. (2.65) vanishes and the fluctuations in the field diverges. It can be shown that this will happen for any $v(z)$ that does not go smoothly to zero where $S'(z)$ is zero. In order to avoid these divergences, in the simulations that are to be presented in Sec. III, we choose a function $v(z)$ that is close to \tilde{z} but becomes flat at $\tilde{z} = \pm \pi/2$.

Validity of the nonlinear feedback Hamiltonian

The same conditions as derived above also apply in this case as for the case of linear feedback, but now we have to consider the extra approximation of using the linearized expression for the nonlinear feedback (2.50). In order to con-

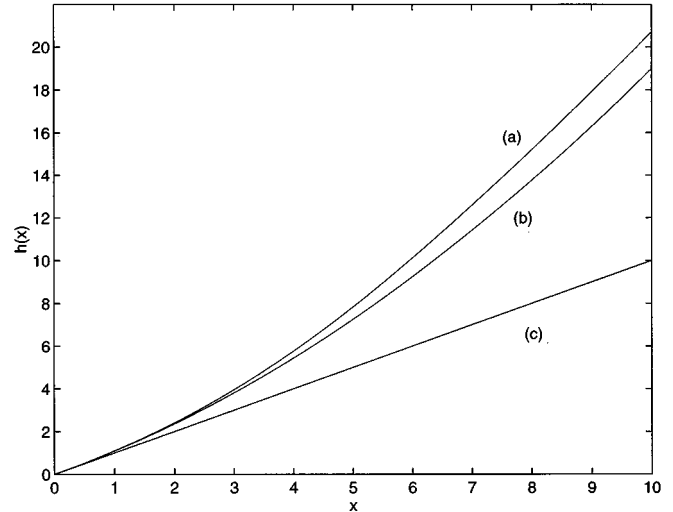


FIG. 3. (a) Plot of the function h given in Eq. (2.78) for $\alpha=10$. (b) Plot of the quadratic approximation to this for small x given in Eq. (2.80), along with (c) the form of h for linear feedback. Both h and x are unitless.

sider this we need to know just how nonlinear the function $h(x)$ is. Up until now we have used only the implicit definition of this function (2.61), which for the case $v(z) = \tilde{z}$ and $r = 1/12$ becomes, for $|z| \leq \pi/2$,

$$h\left(\frac{\alpha}{3}\sin^2 z \sqrt{\frac{z}{\sin z \cos z}}\right) = \alpha \sqrt{\frac{z}{\sin z \cos z}} - \alpha. \quad (2.78)$$

In Fig. 3 we have plotted this function for the case $\alpha=10$. Now we can use this implicit expression to get an approximate explicit expression for $h(x)$ by expanding both sides in powers of z :

$$h\left(\frac{\alpha}{3}[z^2 + O(z^6)]\right) = \alpha[z^2/3 + z^4/10 + O(z^6)]. \quad (2.79)$$

Thus, for x small compared to α , we find that

$$h(x) \approx x + \frac{9x^2}{10\alpha}. \quad (2.80)$$

This is also shown of Fig. 3 and appears to be quite close to the true function over the range of interest.

Using this expression, the linearization of $h(x)$ is the approximation of

$$\bar{x} + \delta x(t) + \frac{\xi(t)}{\sqrt{\kappa}} + \frac{9}{10\alpha} \left(\bar{x} + \delta x(t) + \frac{\xi(t)}{\sqrt{\kappa}} \right)^2 \quad (2.81)$$

by

$$\bar{x} + \delta x(t) + \frac{\xi(t)}{\sqrt{\kappa}} + \frac{9}{10\alpha} \left(\bar{x}^2 + 2\bar{x}\delta x(t) + 2\bar{x}\frac{\xi(t)}{\sqrt{\kappa}} \right). \quad (2.82)$$

This is valid only if we consider averaging the noise over a time t_3 and then ignoring the term

$$\frac{9}{10\alpha} \left(\frac{1}{t_3} \int_0^{t_3} \left[\delta x(t) + \frac{\xi(t)}{\sqrt{\kappa}} \right] dt \right)^2 \approx \frac{9}{10\alpha\kappa t_3}. \quad (2.83)$$

It is valid to ignore this term if it is much smaller than the other terms in Eq. (2.82). Since the signal \bar{x} need not be different from zero, the leading term is of order

$$\left\langle \left(\frac{1}{t_3} \int_0^{t_3} \left[\delta x(t) + \frac{\xi(t)}{\sqrt{\kappa}} \right] dt \right)^2 \right\rangle^{1/2} \approx \frac{1}{\sqrt{\kappa t_3}}. \quad (2.84)$$

Thus we require

$$\frac{1}{\sqrt{\kappa t_3}} \gg \frac{9}{10\alpha\kappa t_3}, \quad (2.85)$$

which gives

$$\frac{1}{t_3} \ll \frac{1200}{81} \omega^2. \quad (2.86)$$

Now, as in the preceding case, in order to be able to average over this time and yet treat the atomic evolution as being Markovian, it is necessary to assume that the time t_3 is small compared to the characteristic time of the atomic motion ω^{-1} . This gives

$$\omega \gg \gg \frac{81}{1200} \approx \frac{1}{15}. \quad (2.87)$$

This is to be compared with the previously derived constraint (2.48) from the linearization of $a^\dagger a$, that $\omega \gg \gg 1/6$. It is therefore apparent that, at least for the atom near the bottom of the well, the linearization of the nonlinearity of the feedback does not impose more of a constraint on the classicality of the problem than that already derived.

E. Linear feedback with optical nonlinearity

It is apparent from Secs. II C and II D that in order to make the effective potential for the atom closer to pseudo-harmonic one wishes to increase the driving (to increase the potential) when the phase of the field shifts (due to the presence of the atom away from a node). In terms of the field quadratures, one wishes to increase the driving of the amplitude quadrature y in proportion to the displacement of the phase quadrature x from zero. One way to do this is to measure x indirectly and to feed this back onto the driving. However, it would seem reasonable to expect that one could also achieve this directly, without measurement or feedback, by introducing a nonlinear crystal into the cavity. The nonlinearity required is one that makes the driving of y proportional to the x quadrature, namely,

$$H_\chi = -\frac{\kappa\chi}{4} x^2 = -\frac{\kappa\chi}{4} (a^2 + a^{\dagger 2} + 2a^\dagger a + 1), \quad (2.88)$$

where χ is a dimensionless parameter. This could in principle be achieved using a process of degenerate parametric down-conversion, with an appropriate detuning of the cavity also. In this section we investigate the effect of this optical nonlinearity on our system.

The total Hamiltonian for the system we now take to be $H_{\text{damped}} + H_\chi$. It is still necessary to include damping as in Eq. (2.11) because without it exponential parametric amplification will occur. The equations of motion for the quadratures are

$$\dot{x} = -\frac{\kappa}{2} x - \sqrt{\kappa} \xi(t) + gS(z)y, \quad (2.89)$$

$$\dot{y} = -\frac{\kappa}{2} y - \sqrt{\kappa} \nu(t) + \kappa\alpha + \kappa\chi x - gS(z)x, \quad (2.90)$$

where $b_{\text{in}}(t) = -i\sqrt{\kappa}\alpha/2 + \nu(t)$ as in Eq. (2.7). Ignoring terms of order r^2 as usual, the stationary solutions of these equations are

$$\frac{x}{2} \approx [1 - 4\chi S(z)r]^{-1} [-\xi(t)/\sqrt{\kappa} + \alpha r S(z)], \quad (2.91)$$

$$\frac{y}{2} \approx [1 - 4\chi S(z)r]^{-1} \{ \alpha - [\nu(t) + 2\chi\xi(t)]/\sqrt{\kappa} \}. \quad (2.92)$$

This solution is very similar to those resulting from linear feedback (2.33) and (2.34), with λ replaced by χ . However, there is actually more noise in the y quadrature, with $\xi(t)$ multiplied by 2χ rather than λ . The consequence of this is that the final noise in the atomic Hamiltonian, for the optimal choice of $\chi = 1/2$ and $r = g/\kappa = 1/6$, is larger by a factor $\sqrt{2}$ than that in the linear feedback Hamiltonian (2.43).

On the basis of this result it would not seem worthwhile pursuing the idea of an optical nonlinearity as an alternative to feedback. Although this is true from considering an optical nonlinearity alone, the combination of an optical nonlinearity and linear feedback turns out to give very interesting results. Adding H_χ to H_{damped} but with

$$b_{\text{in}}(t) = \frac{-i\sqrt{\kappa}}{2} \{ \alpha + \lambda[x + \xi(t)/\sqrt{\kappa}] \} + \nu(t) \quad (2.93)$$

as in Eq. (2.28) yields

$$\dot{x} = -\frac{\kappa}{2} x - \sqrt{\kappa} \xi(t) + gS(z)y, \quad (2.94)$$

$$\begin{aligned} \dot{y} = & -\frac{\kappa}{2} y - \sqrt{\kappa} \nu(t) + \kappa\alpha + \kappa\chi x + \kappa\lambda[x + \xi(t)/\sqrt{\kappa}] \\ & - gS(z)x. \end{aligned} \quad (2.95)$$

The approximate stationary solutions are

$$\frac{x}{2} \approx [1 - 4(\chi + \lambda)S(z)r]^{-1} [-\xi(t)/\sqrt{\kappa} + \alpha r S(z)], \quad (2.96)$$

$$\frac{y}{2} \approx \frac{\alpha - [\nu(t) + (2\chi + \lambda)\xi(t)]/\sqrt{\kappa}}{1 - 4(\chi + \lambda)S(z)r}. \quad (2.97)$$

Now the difference between the noise from the optical nonlinearity and the linear feedback is crucial. If we choose the nonlinearity to have the sign opposite to that suggested above, with

$$\chi = -\lambda/2, \quad (2.98)$$

then we can eliminate the noise due to $\xi(t)$:

$$\frac{y}{2} \approx [1 - 2\lambda S(z)r]^{-1} [\alpha - v(t)/\sqrt{\kappa}]. \quad (2.99)$$

Now choosing $2\lambda g = \kappa/3$ as the optimum for feedback, we find

$$F(z) \approx -g \frac{y^2}{4} S'(z) \quad (2.100)$$

$$\approx -\frac{S'(z)}{[1 - S(z)/3]^2} \left[\frac{\omega^2}{2} - \sqrt{\frac{2g\omega^2}{\kappa}} v(t) \right], \quad (2.101)$$

where $\omega^2 = 2g\alpha^2$ as usual. Now since the optical nonlinearity has exactly canceled the noise due to the feedback, the only noise present is that which can be attributed to measurement, as in Sec. II B. This noise can be made arbitrarily small by letting $g/\kappa \rightarrow 0$. Stating this more carefully, we let

$$g/\kappa \rightarrow 0, \quad \alpha \rightarrow \infty, \quad \lambda = -2\chi \rightarrow \infty \quad (2.102)$$

such that

$$\omega^2 = 2g\alpha^2, \quad \kappa = 6\lambda g \quad (2.103)$$

are constants. Then the final atomic Hamiltonian resulting from linear feedback and optical nonlinearity

$$H_{\text{LFON}} = \frac{p^2}{2} + \frac{S(z)}{1 - S(z)/3} \frac{\omega^2}{2} \quad (2.104)$$

contains no noise, only a modified potential. This is a very interesting example of the interplay of quantum noise and nonlinear dynamics, but it would be very difficult to realize experimentally.

III. RESULTS

A. Method of simulation

Numerical methods are used to simulate the evolution of wave functions in potentials modified by the different feedback schemes discussed above. Due to the periodicity of the optical potential, we need only consider one potential well. We consider an atomic beam that is initially perfectly well collimated with a well-defined velocity. For simplicity, we have ignored effects due to angular and velocity distributions of the initial atomic beam. These effects are covered well, in a classical sense, by McClelland [4]. The motion can be treated classically in a direction perpendicular to the standing wave, but must be treated quantum mechanically parallel to the standing wave. For the cavity field far detuned from the atomic resonance, the probability of an atomic transition between the ground and an excited state is small. We can therefore ignore incoherent effects and simulate only the coherent

evolution of the wave packet as is done by Janicke and Wilkens [16]. Since we are studying channeling, we cannot neglect the kinetic-energy term in the Hamiltonian (which is done in the Raman-Nath regime [13,17]). Instead we use the split operator method to evolve the wave function with time. We begin with the normalized plane-wave wave function Ψ , given by

$$\Psi(z) = \begin{cases} 1/\sqrt{\pi} & \text{for } -\pi/2 \leq z < \pi/2 \\ 0 & \text{otherwise.} \end{cases} \quad (3.1)$$

In addition to considering four cases of feedback, we consider two different cross-section profiles for the standing wave. First, a step profile in which the intensity is effectively turned on sharply at $t=0$ and turned off sharply at the focal time. Second, a half-Gaussian profile case in which the light intensity is increased with a Gaussian dependence, reaching its maximum at the deposition (focal) time. This situation is more physically realistic since a laser beam typically has a Gaussian intensity cross section.

1. Split operator method

If we write our Hamiltonian as

$$H = \frac{p^2}{2} + V(z), \quad (3.2)$$

where V is a position-dependent potential, then the time evolution operator that evolves the wave function by time t is given by

$$U(t) = \exp \left[-i \left(\frac{p^2}{2} + V(z) \right) t \right]. \quad (3.3)$$

For small t we can write

$$U(t) \approx \exp \left[-i \frac{p^2}{2} t \right] \exp[-iV(z)t]. \quad (3.4)$$

This equation would be exact if the commutator of p^2 and V were zero, but it is not. This form of the split operator method is thus only accurate to first order in t , since it ignores terms of order t^2 and above, which involve the commutator of p^2 and V . The split operator method is superior to expanding $U(t)$ to first order in t because it evolves the state unitarily, so that the norm of the wave function remains constant to all orders in t . Higher-order split operator methods also exist [18].

To propagate the wave function numerically by a small time increment δt , we multiply the wave function in position space by the factor $\exp[-iV(z)\delta t]$. We then take the Fourier transform of the result giving a wave function in the momentum representation. Multiplying by $\exp[-ip^2\delta t/2]$ and taking the inverse Fourier transform returns us to a position space wave function evolved by time δt . This is the essence of the split operator method used in the simulations here. For the noisy potentials, we propagate many wave functions through the cavity and average over the results.

If we consider the Hamiltonian given by Eq. (2.5)

$$H = \frac{p^2}{2} + \frac{\omega^2}{2} S(z), \quad (3.5)$$

the error ϵ introduced per step δt by this form of the split operator method is

$$\epsilon = \left| \exp \left[-i \left(\frac{p^2}{2} + \frac{\omega^2}{2} S(z) \right) \delta t \right] - \exp \left(-i \frac{p^2}{2} \delta t \right) \exp \left(-i \frac{\omega^2}{2} S(z) \delta t \right) \right| \quad (3.6)$$

$$\approx \frac{1}{8} \omega^2 (\delta t)^2 [[p^2, S(z)]]. \quad (3.7)$$

So the total error ϵ_{total} in propagating by a given time is

$$\epsilon_{\text{total}} = (\text{number of steps}) \times (\text{error per step}) \quad (3.8)$$

$$\sim \frac{1}{\omega \delta t} \omega^2 (\delta t)^2 = \omega \delta t. \quad (3.9)$$

So, for the propagation to stay within a given error bound, the time increment for the simulations must scale as

$$\delta t \sim \frac{1}{\omega}. \quad (3.10)$$

This means that the number of steps required to fully propagate a wave function up to the focal time (approximately $\pi/2\omega$) is approximately constant with ω .

However, in performing numerical simulations, we need to account for the fact that the number of energy levels in the well varies as ω . The spatial period of wave functions describing particles in an harmonic oscillator varies inversely with the energy level occupied. So, to maintain the same order of resolution of the wave functions for different values of ω , the number of bins in z and p space must scale linearly with ω . This is the case since we can write the wave function for an atom passing through a potential well in the cavity as a linear combination of the wave functions for the different levels in the well. Specifically, we require

$$\omega \ll (\text{number of bins}). \quad (3.11)$$

The calculation time for propagating wave functions therefore scales linearly with ω .

2. Form of the nonlinear feedback

As was discussed at the end of Sec. II D, we need to choose an approximation to the pseudoharmonic potential that becomes flat at $z = (n + 1/2)\pi$. This is necessary to ensure that the noise terms in the Hamiltonian remain finite. To do this, we use the analysis of Sec. II D 2, in which we derive a quadratic approximation (2.80) for the nonlinear feedback function $h(x)$ in the case $v(z) = \tilde{z}$. This approximation is useful not only for establishing the range of validity of the nonlinear feedback Hamiltonian in this singular case; it can also be used as the feedback function in its own right as a way of avoiding the singularity in the noise. That is to say,

we can assume that $h(x)$ is given by the quadratic (2.80) and then determine a $v(z)$ from it that will smoothly go to zero at $z = \pi/2$.

We proceed using Eq. (2.61), which gives the following equation for $f(z)$:

$$\frac{1}{3} S(z) f(z) + \frac{1}{10} [S(z) f(z)]^2 = f(z) - 1, \quad (3.12)$$

which has the meaningful solution

$$f(z) = \frac{1 - \frac{1}{3} S(z) - \sqrt{[1 - \frac{1}{3} S(z)]^2 - \frac{2}{5} [S(z)]^2}}{\frac{1}{5} [S(z)]^2}. \quad (3.13)$$

From this, $v(z) = \sin z \cos z [f(z)]^2$ may be easily found and verified to go smoothly to zero at $z = \pi/2$. The deterministic potential $V_0(z) = \int_0^z d\zeta 2v(\zeta)$ of Eq. (2.72) is then found numerically and is shown in Fig. 1(b).

3. Theory for the Gaussian profile

In order to simulate channeling for standing waves with a Gaussian dependence, we need to be able to modify the theory to deal with time-dependent potentials. The Hamiltonians derived in Sec. II are for the step profile case, but can easily be applied to the Gaussian profile situation by making a simple substitution. In the case of no feedback, the light intensity is modified as

$$\sin^2 z \rightarrow (\sin^2 z) e^{-\beta t^2}, \quad (3.14)$$

where β is a parameter to be determined. In practice, β is calculated numerically to be such that the spread parameter (defined below) has its minimum value at the peak of the Gaussian (where $t=0$). We note that the intensities of the Gaussian and step cases coincide at the Gaussian peak (surface of the substrate).

With feedback, the same procedure works. That is to say, everywhere that $S(z)$ appears it is replaced by $S(z) e^{-\beta t^2}$. For linear feedback, this may be done directly in the Hamiltonian (2.43). For nonlinear feedback it must be done in the equation for $f(z)$ [Eq. (3.13)], which then feeds into the Hamiltonian (2.72).

B. Measures of localization

It is important to have an appropriate measure to compare the sharpness of peaks. The full width at half maximum (FWHM) measurement of peak widths is not particularly useful here, due to the presence of fine structures in the atomic distributions. It is only near the focal times that there is clearly one main peak for which the FWHM method can satisfactorily be applied. The use of the FWHM would not allow us to consider how the position distribution evolves as the atoms pass through the standing wave. Standard deviation is not an ideal measure of localization either, as it does not take into account the periodic nature of the atomic distribution.

Instead we develop a scheme motivated by this periodicity of the deposited atom peaks. For a position probability distribution of atoms, deposited on the substrate, given by the function $P(z)$, where $P(z)$ is normalized so that

$$\int_{-\infty}^{\infty} P(z) dz = 1, \quad (3.15)$$

we define a measure Φ_{spread} as

$$\Phi_{\text{spread}} = 1 - \left(\int_{-\infty}^{\infty} P(z) \cos 2z \, dz \right)^2. \quad (3.16)$$

This measure of localization has the useful limits

$$\Phi_{\text{spread}} = \begin{cases} 0 & \text{for perfect localization} \\ 1 & \text{for a flat probability distribution.} \end{cases} \quad (3.17)$$

For atomic distributions well localized about the nodes of the standing wave, spread is approximately proportional to the variance of z , $\text{var}(z)$, where the mean is zero

$$\Phi_{\text{spread}} \approx 1 - \left(\int_{-\infty}^{\infty} P(z) (1 - 2z^2) dz \right)^2 \quad (3.18)$$

$$\approx 4 \text{var}(z). \quad (3.19)$$

This spread measurement gives more weight to the central region of the peak. It allows us to better distinguish between different distributions. Furthermore, in this physical situation, we are not laying down a single line, but a series of parallel lines. This measure of the position distribution has the advantage that it can be applied to a series of parallel lines, separated by $\Delta z = \pi$, equally as well as to a single line. Spread has the additional favorable property that a plot of spread against ω asymptotes horizontally for large ω . This property allows us to compare different feedback schemes more easily, as is discussed below in Sec. III C. Spread is recorded at the time at which it is a minimum (i.e., the optimum focal time).

Optimum focal time

We have shown that near the nodes of the laser standing wave, the Hamiltonian is well approximated by that of a harmonic oscillator Eq. (2.6). Making this approximation, we would expect the optimum focal time to be equal to one-quarter of the natural period of the harmonic oscillator. As discussed in Sec. II A, this is the time at which all atoms of zero initial transverse momentum would be localized at $z=0$, independent of their initial positions. The true optical potential, of course, is only approximately harmonic, and we need to make a correction to the focal time for this anharmonicity. It turns out that this correction is not small.

Typical results are shown in Fig. 4. We see that, by the spread criterion, the optimum focal time for the case with no feedback is approximately 0.36 oscillator periods (for $\omega = 100 \text{ s}^{-1}$). This is a significant correction to the harmonic prediction of 0.25 periods. It is clearly not reasonable to compare results at the harmonic-oscillator focal time, since this would reflect not only the best localization achievable by different feedback schemes but the focal time for each method. Such a comparison would be biased in favor of potentials close to harmonic. Instead we record values of spread at the optimum focal time for the particular potential experienced by an atom. This time is determined numerically.

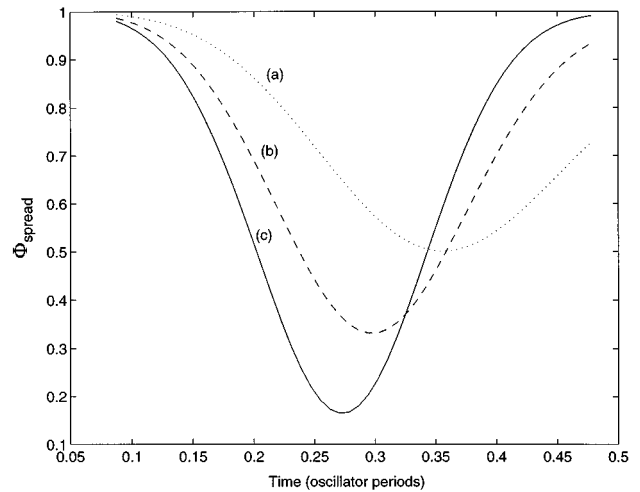


FIG. 4. Diagram of the evolution with time of the spread of the atomic wave functions. The time is in units of the natural period of the harmonic approximation to the potential. Results for $\omega = 100 \text{ s}^{-1}$ are shown for (a) no feedback, (b) linear feedback, and (c) nonlinear feedback. Better localization is achieved for potentials that are closely harmonic. The optimum focal time tends to one-quarter of a period as the feedback is increased.

These results display all the features we would expect. As the potential becomes more closely harmonic, not only does the optimum localization improve, but the focal time approaches one-quarter of a period, the result predicted for a harmonic oscillator. Also evident here is the periodic focusing and defocusing of the atomic wave function, which is characteristic of channeling. Of course, these results depend on how we quantify the localization of the atoms. However, an investigation of different schemes of measurement reveals that all the same qualitative features appear for all reasonable measures such as FWHM, peak height, and standard deviation.

C. Comparison of results

The step and Gaussian profile cases are treated separately. Results for different sorts of feedback are compared by plotting spread against ω (a measure of the well depth), as shown in Figs. 5 and 6. All values of spread are recorded at the optimum focal time. In each of the figures the results for nonlinear, linear, and no feedback are plotted, where the noise has been set to zero. These serve as a comparison to the noisy results. The curves shown for linear feedback with no noise are the results arising from linear feedback with optical nonlinearity Eq. (2.104). In this case, as discussed in Sec. II E, we achieve a modified potential with no noise. Displayed on the same graphs are the results with noise included. For the noisy potentials, we averaged over the wave functions until the standard deviation in $\int_{-\pi/2}^{\pi/2} P(z) \cos 2z \, dz$ was less than 1%.

For no feedback, we would expect there to be no noise since we are not modifying the potential. These noise-free results for no feedback can be seen in Figs. 5(a) and 6(a). Also displayed, for comparison, are noisy results for no feedback. The noise in this case is purely back-action noise in-

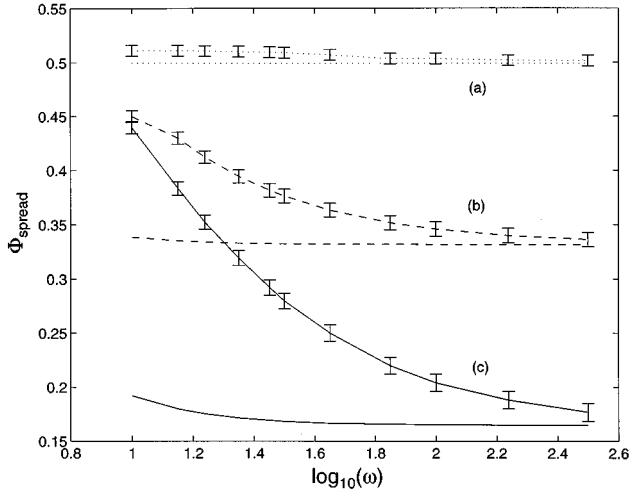


FIG. 5. Diagram showing the variation of spread with ω (in units s^{-1}) for a step profile standing wave. Noisy and noise-free results are compared for (a) no feedback, (b) linear feedback, and (c) nonlinear feedback. The error bars shown on the noisy results are \pm one standard deviation (i.e., $\pm 1\%$, as discussed in Sec. III C).

roduced when we measure the atom's position. The noisy results represent measuring the atom's position but not feeding this information back. For the noise-free results, we are not even monitoring the atom's position as it passes through the standing wave. The only unphysical case shown in these results is that for nonlinear feedback with no noise.

We need to be cautious about making comparisons between the different feedback cases for the following reason. For a given value of ω , the depth of the potential wells (and hence the number of energy levels) is not the same for the three cases of feedback. It therefore seems unfair to compare the value of spread for the three cases at the same value of ω . Fortunately, however, the problem is alleviated for large

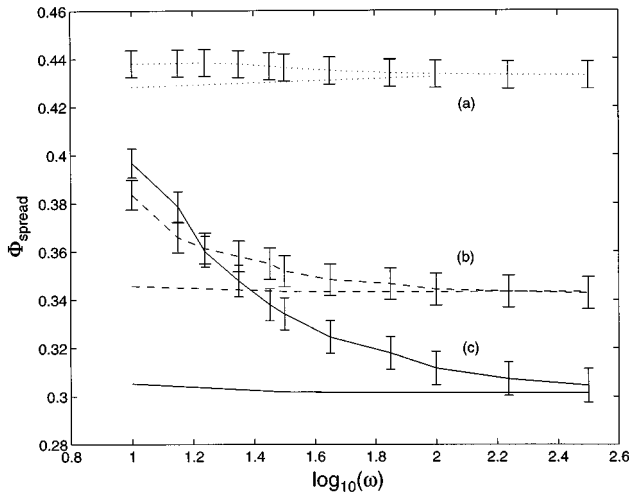


FIG. 6. Variation of spread with ω (in units s^{-1}) for a Gaussian profile standing wave for (a) no feedback, (b) linear feedback, and (c) nonlinear feedback. The error bars shown on the noisy results are \pm one standard deviation (i.e., $\pm 1\%$, as discussed in Sec. III C).

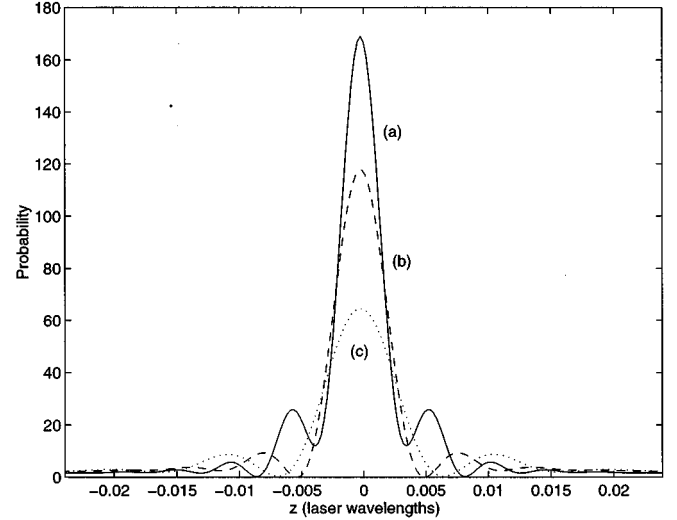


FIG. 7. Comparison of the atomic deposition profiles with no noise for $\omega = 100 s^{-1}$ at the optimum focal times for (a) nonlinear feedback, (b) linear feedback, and (c) no feedback. The profiles are shown as a function of position along the cavity axis z (in units of the laser wavelength).

ω (the region where our theory is valid) since spread varies slowly with ω in this region. This is another advantage of the spread measurement over some of the other measurement schemes. The most notable feature of these results is that, for sufficiently large values of ω , nonlinear feedback gives better localization than linear feedback which, in turn, gives better localization than no feedback. This is true for both Gaussian and step profile cases.

We see also that the noisy quantum results tend to the noise-free results for large ω . This is what we would expect. For each time step δt , the noise is given by an independent Gaussian distributed random variable with mean $\mu = 0$ and variance $\sigma^2 = 1/\delta t$. Given that the number of time steps scales as ω (see Sec. III A), the signal-to-noise ratio R_{SN} for the potential varies with ω approximately as

$$R_{SN} \sim \sqrt{\omega}. \quad (3.20)$$

So the noise becomes less important as ω tends to infinity. To give an indication of their shape and scale, typical deposition peaks are compared in Fig. 7.

1. Comparison of step and Gaussian cases

By comparing Figs. 5 and 6, we see that for nonlinear feedback the step profile gives improved localization over the Gaussian profile, but for no feedback, the Gaussian case gives better localization. This is what we would expect intuitively as is demonstrated by the following argument.

The standing light wave serves the dual purpose of providing the optical potentials, which channel the atoms, and allowing us to monitor the atom's position by making phase measurements. For the Gaussian case, the coupling of the phase measurement to the feedback is set at its ideal value for the intensity at the maximum of the Gaussian. When an atom enters the standing wave, the intensity is low and so the phase shifts are small. In the low-intensity wings, the feed-

back for an atom near an antinode would be the same as for an atom much closer to a node, near the Gaussian maximum. As the intensity increases, the feedback improves, reaching its optimum value at the Gaussian maximum. For nonlinear feedback, the step profile is superior since, in this case, an atom experiences the optimum feedback throughout its passage through the cavity. On average, therefore, the potential experienced by an atom in the step case is more closely harmonic than for the Gaussian case.

Of course, if we knew what part of the Gaussian the atom was in at any given time, we could arrange to have a time-varying coupling between the phase shift and the feedback. By matching the coupling with the Gaussian dependence of the standing wave, this would allow atoms in the Gaussian case to experience optimum feedback throughout their passage through the cavity. Knowledge of the atom's whereabouts could be achieved by using a shutter system on the atomic beam combined with knowledge of the longitudinal velocity of the atoms. The calculations for this situation, however, are more complicated and are not considered here.

By comparison, for no feedback, the Gaussian case is superior. This is understood since in the low-intensity wings of the Gaussian, the optical forces are small. The time taken by an atom to move a given small distance δz from near an antinode towards a node is longer than for the step case. However, the momentum imparted to the atom in making this translation is less than for the step case. By the time the atom reaches the high-intensity and relatively strong optical forces, it is already partially localized in a region where the potential is more closely harmonic. The momentum given to the atom in achieving this situation is less than that for the step case. In some sense, we can consider the velocity distribution brought about by the anharmonic part of the potential to be less for the Gaussian case than for the step profile case. The anharmonicity of the potential has less of a disruptive effect in the Gaussian case.

2. Comparison in the classical limit

In considering the results in Figs. 5 and 6 we need to be aware that we cannot give much emphasis to the results for small values of ω . The Hamiltonians derived in Sec. II do not hold in the strongly quantum regime. In this region, the condition $\omega \gg 1/6$ breaks down. It seems reasonable to consider that $\omega > 100$ satisfies these two conditions and so the results shown are valid.

Our results for large ω show that, even when noise is taken into account, the use of feedback systems improves the localization we can achieve. The noisy quantum results tend to the noise-free results for large ω . A calculation of the classical limits (not shown) gives about the same value, as expected by the correspondence principle.

IV. EXPERIMENTAL PARAMETERS

Our aim in this paper was to compare the localization able to be achieved by different theoretical schemes. We should, however, consider how well our simulations would describe experimental results. In this section we show to what extent the approximations we have made are valid and also consider other effects such as spontaneous emission and feedback delay times.

We consider the example of rubidium atoms for which the resonant wavelength for the $5S_{1/2} \rightarrow 5P_{3/2}$ transition is $\lambda = 780$ nm and the linewidth is $\Gamma = 37.7$ MHz. Using the parameters proposed by Treussart *et al.* [19] gives a maximum one photon Rabi frequency of

$$\Omega_{\max} = 4.4 \times 10^8 \text{ Hz.} \quad (4.1)$$

As above, we wish to use atom optics units defined by

$$\hbar = M = k = 1. \quad (4.2)$$

The conversion between these units and SI units is found by considering the recoil energy of an atom that has absorbed or emitted a photon ($M = 85$ amu for rubidium)

$$\omega_{\text{recoil}} = \frac{E_{\text{recoil}}}{\hbar} = \frac{\hbar k^2}{2M} = \frac{1}{2} \approx 24 \text{ kHz,} \quad (4.3)$$

so

$$1 \approx 48 \text{ kHz.} \quad (4.4)$$

In these units $\Omega_{\max} \approx 10^4$ and $\Gamma \approx 800$.

In the derivations above, we have the constraints

$$\kappa \gg \omega, \quad (4.5)$$

$$\frac{g}{\kappa} = \frac{1}{12} \quad (4.6)$$

and the definitions

$$g = \frac{\Omega^2}{\Delta}, \quad (4.7)$$

$$\omega^2 = 2g|\alpha|^2. \quad (4.8)$$

Substituting Eqs. (4.6) and (4.8) into Eq. (4.5) gives the condition

$$6\sqrt{2g} \gg \alpha. \quad (4.9)$$

In all the following, we use Ω_{\max} for Ω . In the derivation of the Hamiltonians, the adiabatic elimination of the field variables gives us the additional requirement

$$\Omega_{\max} \alpha \ll \Delta. \quad (4.10)$$

We take

$$\frac{\Omega_{\max} \alpha}{\Delta} = \frac{1}{10}, \quad (4.11)$$

so from Eq. (4.7),

$$g = \frac{\Omega_{\max}^2}{\Delta} = \left(\frac{\Omega_{\max} \bar{\alpha}}{\Delta} \right) \frac{\Omega_{\max}}{\alpha} = \frac{10^3}{\alpha}. \quad (4.12)$$

To satisfy both Eqs. (4.9) and (4.12), we choose $\alpha = 10$ and $g = 100$. These values give

$$\omega = \sqrt{2g} \alpha = 140 \quad (4.13)$$

and a spontaneous decay rate γ of

$$\gamma = \Gamma \left(\frac{\Omega_{\max} \alpha}{\Delta} \right)^2 \approx 8, \quad (4.14)$$

and so the assumption $\gamma \ll \omega$ (that is, that the rate of spontaneous emission is much less than the frequency of oscillation of an atom in the potential) may also be justified.

Since atoms need to interact with the light field for a time approximately equal to one-quarter of an oscillation period, this gives an interaction time τ of

$$\tau \approx \frac{\pi}{2\omega} \approx 2 \times 10^{-7} \text{ s}. \quad (4.15)$$

This interaction time defines the ratio of the cavity width to the atomic beam longitudinal velocity. For a cavity mode width of order 10^{-6} m (required for the large coupling Ω_{\max}), the beam velocity would have to be of order 10 m/s, which presents no great problems. Finally, for successful feedback, we require a feedback loop delay that is much shorter than the interaction time. This seems reasonable as experimentalists can certainly achieve loop delays smaller than 10^{-8} s [15].

V. CONCLUSION

Our results show that the use of feedback systems allows better atom localization to be achieved than in a system without feedback. Furthermore, nonlinear feedback is an improvement over linear feedback. Quantitatively, for a light wave with a rectangular profile, the variance [20] of the final atomic position in the case of nonlinear feedback can be less than half of that in the case of no feedback. An improvement is also evident for a half-Gaussian light profile, but it is less dramatic.

Despite these promising results, it is not clear that this

method would be useful for lithographic purposes since, to measure the position of an atom, there can be only one atom in the light field at any time (see Ref. [5]). This limits us to a typical deposition rate of only 10^6 atoms per second, which may be too slow for practical purposes.

Also, in deriving our theory we have neglected terms that, when one examines realizable experimental parameters, are found to be of only marginal smallness. For example, the neglect of spontaneous emission relies on the approximation that $8 \ll 140$. To a first approximation it seems reasonable to ignore these complicating effects. A more accurate simulation, however, would need to take these into account. This would include dropping the assumption of Markovicity, which would probably entail using an alternative quantum theory of feedback, based on quantum trajectories [7,8]. In order to describe experimental results, simulations would need to begin with atoms with some velocity distribution in both the transverse and longitudinal directions and to model accurately the intensity profile of the cavity mode.

In summary, we have demonstrated that, by using a feedback scheme, we can successfully manipulate the motion of a single atom in a standing wave. Although the uses for such a scheme are unclear at this stage, it is nonetheless an interesting application of quantum measurement theory and the quantum theory of feedback to atom optics. There may well be other areas of atom optics besides channeling, such as cooling and trapping, in which similar feedback schemes could prove useful.

ACKNOWLEDGMENTS

We would like to acknowledge discussions with M.J. Collett and S.M. Tan. This project was supported by the Marsden Fund of the Royal Society of New Zealand and by the University of Auckland Faculty of Science.

-
- [1] J. Dalibard and C. Cohen-Tannoudji, *J. Opt. Soc. Am. B* **2**, 1707 (1985), and references therein.
- [2] C. Salomon, J. Dalibard, A. Aspect, H. Metcalf, and C. Cohen-Tannoudji, *Phys. Rev. Lett.* **59**, 1659 (1987).
- [3] J.J. McClelland, R.E. Scholten, E.C. Palm, and R.J. Celotta, *Science* **262**, 877 (1993).
- [4] J.J. McClelland, *J. Opt. Soc. Am. B* **12**, 1761 (1995).
- [5] Pippa Storey, Matthew Collett, and Daniel Walls, *Phys. Rev. Lett.* **68**, 472 (1992); *Phys. Rev. A* **47**, 405 (1993).
- [6] R. Quadt, M.J. Collett, and D.F. Walls, *Phys. Rev. Lett.* **74**, 351 (1995).
- [7] H.M. Wiseman, *J. Mod. Phys. Lett. B* **9**, 629 (1995).
- [8] H.M. Wiseman, *Phys. Rev. A* **49**, 2133 (1994); **49**, 5159(E) (1994); **50**, 4428 (1994).
- [9] D.F. Walls and G.J. Milburn, *Quantum Optics* (Springer, Berlin, 1994).
- [10] Strictly, of course, the eigenstates of the Hamiltonian (2.5) are delocalized and the energies occur in bands, but the arguments here still apply.
- [11] F. Haake, *Quantum Signatures of Chaos* (Springer-Verlag, Berlin, 1991).
- [12] C.W. Gardiner and M.J. Collett, *Phys. Rev. A* **31**, 3761 (1985).
- [13] C.W. Raman and N.S. Nath, *Proc. Ind. Acad. Sci.* **2**, 406 (1933).
- [14] H.P. Robertson, *Phys. Rev.* **34**, 163 (1929).
- [15] M.S. Taubman, H.M. Wiseman, D.E. McClelland, and H.-A. Bachor, *J. Opt. Soc. Am. B* **12**, 1792 (1995).
- [16] U. Janicke and M. Wilkens, *J. Phys. (France) II* **4**, 1975 (1994).
- [17] C. Henkel, J.-Y. Courtois, and A. Aspect, *J. Phys. (France) II* **4**, 1955 (1994).
- [18] J.A. Fleck, Jr., J.R. Morris, and M.D. Fleit, *Appl. Phys.* **10**, 129 (1976).
- [19] F. Treussart *et al.*, *Opt. Lett.* **19**, 1651 (1994).
- [20] Technically, the ‘‘spread’’ rather than the variance: see Sec. III B.